Semiconductivity in the double-zigzag-chain complex oxide RE$_2$Ba$_2$CuPtO$_8$ (RE identical to Y, Er, Ho)

LETTER TO THE EDITOR

Semiconductivity in the double-zigzag-chain complex oxide $RE_2Ba_2CuPtO_8$ ($RE \equiv Y$, Er, Ho)

N Toyota†‡, P Koorevaar†, J van der Berg†, P H Kes†, J A Mydosh†, T Shishido§, Y Saito§, N Kuroda§, K Ukei§, T Sasaki§ and T Fukuda§

† Kamerlingh Onnes Laboratorium, Rijksuniversiteit te Leiden, Leiden 2300RA, The Netherlands
§ Institute for Materials Research, Tohoku University, Sendai 980, Japan

Abstract. The temperature dependence of electrical conductance has been measured on single crystals of the newly discovered oxide compound $RE_2Ba_2CuPtO_8$ ($RE \equiv Y$, Er, Ho). This Pt- containing oxide is orthorhombic and has a characteristic double-zigzag chain of $-O^{2-}-Pt^{4+}-O^{2-}-Cu^{2+}-O^{2-}-$ in columns running parallel to the b axis, which is the growth direction of the rectangular-shaped long-bar single crystals. All these compounds are found to be semiconductors with energy gaps of about 0.2–0.4 eV. They exhibit conductances proportional to $\exp(-T^{-1/2})$ rather than the thermally activated $\exp(-T^{-1})$ dependence. Such behaviour is discussed in terms of two models, namely, one-dimensional variable-range hopping and the lattice-vibration-induced band-broadening effect.

Recently there has been renewed interest in the physical properties of non-super-conducting complex oxides whose crystal structures are different from, but somewhat related to, the high-T_c layered oxides. One of these compounds is Pt-containing $RE_2Ba_2CuPtO_8$ with $RE \equiv Y$, Er and Ho. They were discovered [1] as a by-product in the single-crystal growth process of '1–2–3' compounds via the flux method using a Pt container. Crystals recovered were long rectangular-shaped single crystals grown near the container wall. The crystal structure of this new compound was clarified independently by three different groups [2–4], and found to have a characteristic double-zigzag chain of –O–Pt–O–Cu–O– running parallel to the orthorhombic b axis. In this Letter we study the electronic transport properties of this compound.

The single crystals were grown by the flux method of which detailed descriptions are given in [1] and [5]. The typical size of the as-grown crystals is about (1–0.5) × 0.2 × 0.2 mm³. Conductivity measurements were performed on these small single crystals, in the temperature range between 90 and 380 K, by gluing thin gold wires, 30 μm in diameter, to both ends of the crystals with silver paint (Electrodag 1415). All measurements were carried out in a two-probe configuration since the impedances were so high that a four-probe method was unnecessary. Conductivity was measured with a Keithley 617 electrometer operating at a constant voltage of 1 V. This enabled us to measure impedance up to 10^{13} Ω.

‡ On leave from Institute for Materials Research, Tohoku University, Sendai, to where further correspondence should be sent.
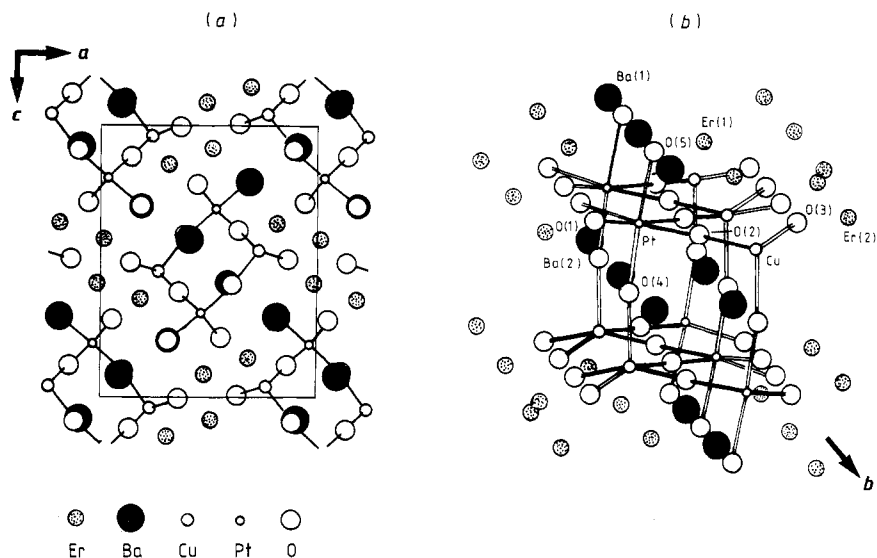
Figure 1. Crystal structure of $Er_2Ba_2CuPtO_8$: (*a*) projection of the structure along the *b* axis; (*b*) perspective view of a double-zigzag chain of Cu, O and Pt and the surrounding Er and Ba ions.

The crystal structure of the present compound, e.g. $Er_2Ba_2CuPtO_8$, is orthorhombic (space group Pcm*n*) with $a = 10.287$, $b = 5.659$ and $c = 13.157$ Å [4]. Y-based [2,3] and Ho-based [6] compounds are isostructural to the Er-based compound, having almost equal lattice constants. Two formula units are included in a unit cell. Figure 1(*a*) and 1(*b*) show, respectively, the projection of the structure along the *b* axis, and the perspective view of a double-zigzag chain of Cu, O and Pt ions with surrounding Er and Ba ions. The anionic neighbours of Pt form distorted octahedra with a Pt–O distance of about 2.0 Å. The Cu ion is surrounded by five oxygen ions forming a distorted square pyramid with a Cu–O distance of 2.0 Å. These PtO_6 octahedra and CuO_5 pyramids are 'corner sharing' and this leads to a double-zigzag chain of –O–Pt–O–Cu–O– running parallel to the *b* axis.

The temperature-dependent conductivity of three single crystals with different RE ions is shown in figure 2, where the logarithmic conductivity is plotted as a function of T^{-1} and $T^{-1/2}$. The data showed no hysteresis in either cooling or heating runs. The higher resistances above 10^{12}–10^{13} Ω were difficult to measure accurately. For each sample, this limited the temperature range available for measurements. As seen in figure 1, a systematic, upward deviation from the T^{-1} dependence occurs; in contrast, a good fit of the data to $T^{-1/2}$ is obtained in every case over several decades of conductivity. That is to say, the logarithmic conductivity is proportional to the inverse square root of temperature

$$\sigma = \sigma_0 \exp[-(T_0/T)^{1/2}]. \tag{1}$$

Here σ_0 and T_0 are constants (see below). Regular thermal-activation-type conductivity

$$\sigma = \sigma_a \exp(-E_g/k_B T) \tag{2}$$

(where σ_a is the conductivity prefactor when $T \to \infty$ and E_g is the activation energy equal to half the energy gap) fails to explain these data. Table 1 lists the values of σ_0 and
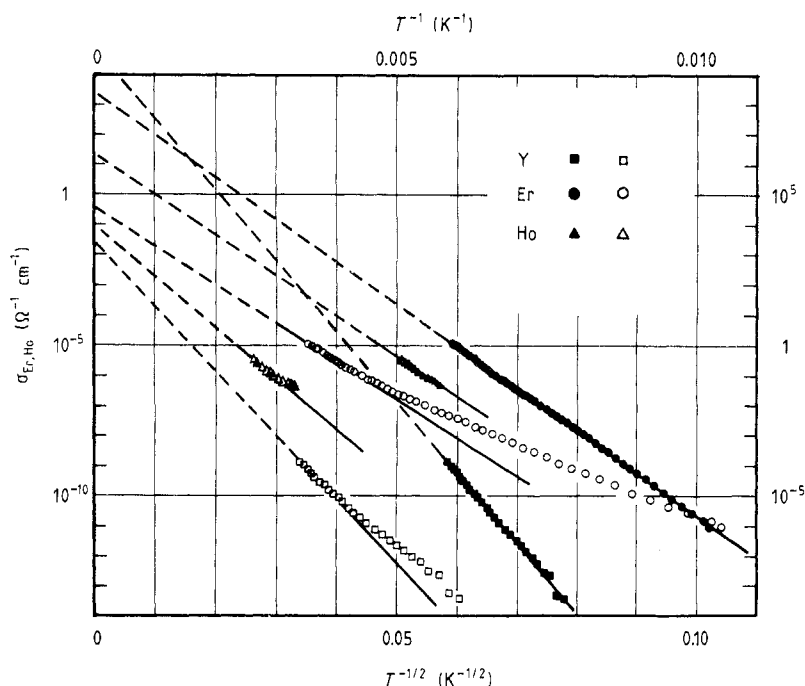
Figure 2. Temperature dependence of conductivity for various $RE_2 Ba_2CuPtO_8$ compounds plotted as logarithmic conductivity against inverse temperature (open symbols) and inverse square-root temperature (full symbols). The straight lines are guides to the eye.

Table 1. Parameters of $RE_2Ba_2CuPtO_8$.

RE ion	$\sigma_0\ (\Omega^{-1}\,cm^{-1})$	T_0 (K)	E_g (eV)	W_T (eV)
Y	10^{10}	1.6×10^5	0.4	0.022
Er	10^{3-4}	4.4×10^4	0.2	0.017
Ho	10^{1-2}	1.0×10^5	—	—

For σ_0 and T_0, see equation (1) in the text.
For E_g and W_T, see equation (4) in the text.

T_0 for each compound under consideration. The magnitude of σ_0 is highly sample-dependent, but T_0 remains practically the same order of magnitude.

It might be reasonable to assume that the zigzag chain as shown in figure 1 should be responsible for the semiconductivity in the present system. Since a quasi-one-dimensional chain is generally sensitive to disorder and has strongly anisotropic lattice vibrations, we discuss the following two theoretical models to explain the characteristic conductivity behaviour expressed by (1).

First, the variable-range hopping conduction originally proposed by Mott [7, 8] should be considered. This theory deals with a disordered system having a finite density of states at the Fermi level. Phonon-assisted electron hopping between localised states leads to conductivity, $\ln \sigma \propto T^{-1/d+1}$ where d denotes the electronic dimensionality of the system. This relation holds for $d = 2$ and 3, but, in quasi-1D systems with finite inter-
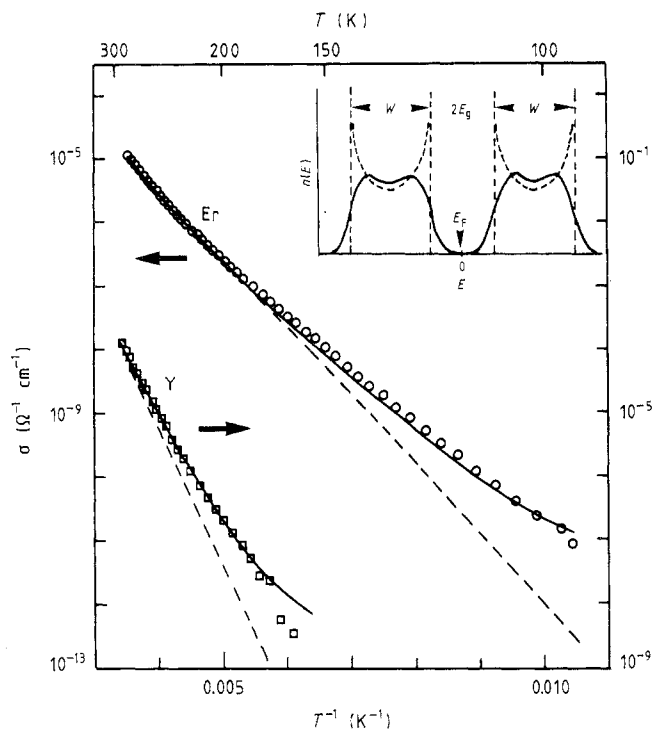
Figure 3. Logarithmic conductivity as a function of inverse temperature for the Er- and Y-based compounds, $RE_2 Ba_2 CuPtO_8$. The full curves are the fit described in the text using the density-of-states model of the lattice-vibration-induced bands shown in the inset. The broken curves are the rigid-lattice contributions.

chain interactions, the exponent is temperature dependent with one half its maximum value [9]. At higher temperatures the hopping distance becomes so short that the inter-chain interaction will be ineffective. At first sight this model seems consistent with our results. However, the variable-range hopping mechanism requires a high degree of structural disorder and a substantial density of states (DOS) at the Fermi level. Consequently, it is questionable to apply this model to the present system, which is highly ordered and single crystalline, as verified by x-ray precession photography and electron-transmission microscopy.

As an alternative, to explain our results that the '$T^{1/2}$' law holds over the several decades of conductivity and a factor three in temperature, we follow recent arguments of Kramer and co-workers [10]. These were successfully used to interpret the conductivity in some organic semiconductors, e.g. $(Et_4 N)[Ni(dmit)_2]$ etc. The inset of figure 3 shows our band model. The bands (broken curves) with high DOS at the band edges, due to the 1D character of the zigzag chain, are split symmetrically with respect to the Fermi level E_F. The band width W is determined by the transfer integral between d(Cu, Pt) and p(O) orbitals. The band gap, $2E_g$, is also illustrated in the figure. When the lattice vibrations are included the bands will be broadened, with a tail that extends far into the gap regions of the rigid lattice, as is shown by the full curve in the figure. Such an effect is due to the lattice-vibration-induced change in the transfer integral, which now modulates the band width, thus leading to the broadening of the bands. In 1D systems

with any amount of disorder, the states in the tailed bands are always localised and we assume the conductivity is solely determined by the variation in carrier number with temperature through Fermi-distribution function $f(E)$. For simplicity, we approximate the density of states $n(E)$ as

$$n(E) = \begin{cases} n_0 & \text{for } E < -E_g \\ n_0 \exp[-(E+E_g)]/W_T & \text{for } -E_g < E < 0 \end{cases} \tag{3}$$

where n_0 is a constant and W_T is the decay width of the exponentially tailed band. The conductivity, which is proportional to the thermally activated carrier number obtained by the integration of $n(E)(1-f(E))$, may be expressed [10] as

$$\sigma = 2e\mu n_0 k_B T[\exp(-E_g/W_T) + \exp(-E_g/k_B T)] \tag{4}$$

where e is the electron charge and μ the mobility. This equation holds under the assumption $E_g > W_T > k_B T$. The second term in (4) represents the usual rigid-band contribution. The first term comes from the contribution of the band tail with W_T which depends on $(k_B T)^{1/2}$. That is to say, because the change in transfer integral caused by lattice vibrations is proportional to the vibrational amplitude, it has a $(k_B T)^{1/2}$ dependence on temperature as long as the lattice remains harmonic at temperatures higher than the Debye temperature. Figure 3 shows the comparison between this theory and data for Er- and Y-based compounds. The full and broken curves indicate, respectively, the total and rigid band contributions. A set of parameters (E_g, W_T) is established to make a best fit. With $E_g = 0.2$–0.4 eV and $W_T = 0.02$ eV at room temperature, which satisfy the above inequality, we obtain a good agreement between data and this model (see the full curve in figure 3).

To check our band model we performed an optical measurement on the Er-based compound at room temperature by using a microscope–spectrometer system. Our microscope limits the wavelength of light to the range between 0.4 and 1.7 μm. The absorption of the crystals with a typical thickness of 0.2 mm is so high over this wavelength range that it is difficult to deduce the absorption spectrum. The reflectivity, however, is as low as 0.1, irrespective of wavelength. These features suggest that an intense absorption band lies near or below 0.5 eV. This band probably arises from the inter-band transition associated with the energy gap of $2E_g$.

We note that antiferromagnetic correlations or orderings of localised spins of Cu^{2+}, Er^{3+} and Ho^{3+} have been observed in the present systems. A charge-neutrality requirement leads to the valence state Pt^{4+}, which has no localised spin, and hence we arrive at a $-O^{2-}-Pt^{4+}-O^{2-}-Cu^{2+}-O^{2-}$ zigzag chain, consistent with the chemical arguments [3]. The presence of a quantum spin localised on Cu sites suggests that the band gap 0.2–0.4 eV obtained above could be a correlation gap or charge-transfer gap in the Mott–Hubbard-like picture applied to 1D zigzag chains. Recently, magnetic and electronic properties similar to the ones obtained here have been reported on Cu- (and/or Pt-) containing, non-superconducting complex oxides such as $Y_2Cu_2O_5$ [11], Y_2BaCuO_5 [12, 13], $Y_2Ba_3Cu_2PtO_{10}$ [14] and $YBa_4Cu_3O_{8.5-9.0}$ [15]. It will be most interesting to ascertain whether these compounds can be understood on the basis of the Mott–Hubbard-like picture, an approach which has been employed extensively for high-T_c oxides.

References

[1] Shishido T, Fukuda T, Toyota N, Ukei K and Sasaki T 1987 *J. Cryst. Growth* **85** 599
[2] Swinnea J S and Steinfink H 1987 *Acta Crystallogr.* C **43** 2436
[3] Laligant Y, Ferey G, Hervieu M and Raveau B 1987 *Europhys. Lett.* **4** 1023
[4] Ukei K, Shishido T and Fukuda T 1988 *Acta Crystallogr.* C **44** 958
[5] Shishido T, Saito Y, Fukuda T, Toyota N, Sasaki T, Iwasaki H and Ukei K 1988 *Japan. J. Appl. Phys.* **27** L1926
[6] Saito Y, Shishido T, Toyota N, Ukei K, Sasaki T and Fukuda T *Int. Conf. Crystal Growth (ICCG-9)* submitted
[7] Mott N F 1968 *J. Non-Cryst. Solids* **1** 1
[8] Mott N F and Davis E A 1979 *Electronic Processes in Non-crystalline Materials* (Oxford: Clarendon) ch 2
[9] Shante V K S 1977 *Phys. Rev.* B **16** 2597
[10] Kramer G J and Brom H B 1988 *J. Phys. C: Solid State Phys.* **21** 6085
[11] Ramakrishna B L, Ong E W and Iqbal Z 1988 *Solid State Commun.* **68** 775
[12] Kojima K, Ohbayashi K, Udagawa M and Hihara T 1987 *Japan. J. Appl. Phys.* **26** L766
[13] Ong E W, Ramakrishna B L and Iqbal Z 1988 *Solid State Commun.* **66** 171
[14] Hibiya T, Nakabayashi Y, Satoh T and Kawamura T 1989 *Japan. J. Appl. Phys.* **28** L63
[15] de Leeuw D M, Mutsaers C A H A, Steeman R A, Frikke E and Zandbergen H W *Physica C* submitted